Corrected 19 March 2021. See full text.

RESEARCH ARTICLE

MULTIPLE SCLEROSIS

A noninflammatory mRNA vaccine for treatment of experimental autoimmune encephalomyelitis

Christina Krienke[1,2], Laura Kolb[1]*, Elif Diken[1]*, Michael Streuber[1], Sarah Kirchhoff[1], Thomas Bukur[1], Özlem Akilli-Öztürk[1], Lena M. Kranz[3], Hendrik Berger[3], Jutta Petschenka[1,4], Mustafa Diken[1,3], Sebastian Kreiter[1,3], Nir Yogev[5,6], Ari Waisman[2,5], Katalin Karikó[3], Özlem Türeci[3,7], Ugur Sahin[1,2,3]†

The ability to control autoreactive T cells without inducing systemic immune suppression is the major goal for treatment of autoimmune diseases. The key challenge is the safe and efficient delivery of pharmaceutically well-defined antigens in a noninflammatory context. Here, we show that systemic delivery of nanoparticle-formulated 1 methylpseudouridine-modified messenger RNA (m1Ψ mRNA) coding for disease-related autoantigens results in antigen presentation on splenic CD11c$^+$ antigen-presenting cells in the absence of costimulatory signals. In several mouse models of multiple sclerosis, the disease is suppressed by treatment with such m1Ψ mRNA. The treatment effect is associated with a reduction of effector T cells and the development of regulatory T cell (T_{reg} cell) populations. Notably, these T_{reg} cells execute strong bystander immunosuppression and thus improve disease induced by cognate and noncognate autoantigens.

Antigen-specific tolerization for the treatment of autoimmune diseases may selectively blunt autoimmunity without compromising normal immune function. In the past decades, various approaches have been studied, including delivery of autoimmune antigens using DNA, synthetic peptides, recombinant proteins, coated nanoparticles, or immunomodulatory cellular therapies [reviewed in (*1*)]. However, clinical translation remained elusive, with largely negative or inconclusive outcomes in human studies, and only a few approaches are in early clinical testing. One impediment is the polyclonal complexity of autoimmune diseases driven by distinctive, diverse autoreactive immune cell repertoires of patients. The interindividual variability requires either personalized treatment tailored for the autoantigenic immune profiles of the patients or therapies that mediate bystander tolerance to suppress both cognate and noncognate autoimmune lymphocytes without broad immune suppression (*2*).

[1]TRON – Translational Oncology at the University Medical Center of the Johannes Gutenberg University gGmbH, Freiligrathstr. 12, Mainz 55131, Germany. [2]Research Center for Immunotherapy (FZI), University Medical Center at the Johannes Gutenberg University, Langenbeckstr. 1, Mainz 55131, Germany. [3]Biopharmaceutical New Technologies (BioNTech) Corporation, An der Goldgrube 12, Mainz 55131, Germany. [4]Cancer Immunology and Immune Modulation, Boehringer Ingelheim Pharma GmbH & Co. KG, Birkendorfer Str. 65, 88397 Biberach an der Riss, Germany. [5]Institute for Molecular Medicine, University Medical Center of the Johannes Gutenberg University, Mainz 55131, Germany. [6]Clinic and Polyclinic for Dermatology and Venereology, University Hospital Cologne, Kerpenerstr. 62, Cologne 50937, Germany. [7]CI3 – Cluster for Individualized Immunointervention e.V., Hölderlinstraße 8, 55131 Mainz, Germany.
*These authors contributed equally to this work.
†Corresponding author. Email: sahin@uni-mainz.de

The physiological induction and maintenance of peripheral tolerance is based on the presentation of self-antigens by lymphoid antigen-presenting cells (APCs) with low-level surface expression of costimulatory molecules, such as CD86. We sought to develop a therapeutic approach that would emulate natural mechanisms of immune tolerance. We recently introduced a liposomal formulation for systemic delivery of mRNA-encoded vaccine antigens (mRNA-LPX) into lymphoid tissue-resident CD11c$^+$ APCs (*3*). mRNA vaccination induces strong type 1 T helper (T_H1) cell responses driven by high levels of interferon-α (IFN-α), released from APCs upon Toll-like receptor (TLR) signaling (*3*). Replacement of uridine (U) by incorporation of 1-methylpseudouridine (m1Ψ) during in vitro transcription and subsequent removal of double-stranded mRNA contaminants is known to abrogate TLR7-triggering activity and to reduce inflammatory properties of single-stranded mRNA (*4*–*6*). We hypothesized that the use of such nucleoside-modified, purified mRNA (m1Ψ mRNA) for in vivo delivery of autoimmune disease target antigens into CD11c$^+$ APCs in a noninflammatory context would enable systemic tolerogenic antigen presentation in lymphoid tissues.

Noninflammatory delivery of antigen-encoding m1Ψ mRNA into the spleen expands antigen-specific CD4$^+$ regulatory T cells

To test this hypothesis, we engineered nanoparticle-formulated mRNA-LPX (herein referred to as mRNA) consisting of nonimmunogenic (m1Ψ) or immunogenic (U) mRNA complexed with liposomes that lack inherent adjuvant activity. In a first experiment, mRNA coding for the reporter gene firefly luciferase (LUC) or saline as control was administered intravenously into albino C57BL/6 mice, and the translation and expression of the LUC protein was assessed.

In line with previous reports, administration of U mRNA led to strong activation of CD11c$^+$ APCs and lymphocytes, and secretion of high levels of IFN-α (Fig. 1, A to C, and fig. S1, A and B). By contrast, we did not observe secretion of IFN-α or other inflammatory cytokines or significant activation of CD11c$^+$ APCs, CD8$^+$ and CD4$^+$ T cells, or natural killer (NK) and B cells in m1Ψ mRNA–treated mice (Fig. 1, A to C, and fig. S1, A and B). Notably, translation of LUC was profoundly higher and prolonged in m1Ψ mRNA–treated animals (Fig. 1, D and E). These findings suggest that m1Ψ mRNA is suitable for noninflammatory delivery of proteins into splenic CD11c$^+$ APCs.

To study the effects of m1Ψ mRNA in an autoimmune disease, we chose experimental autoimmune encephalomyelitis (EAE), a clinically relevant mouse model of multiple sclerosis (MS), in which we previously demonstrated tolerance induction by selectively expressing MOG_{35-55}, the epitope of myelin oligodendrocyte glycoprotein, in dendritic cells (DCs) (*7*). We assessed the effect of antigen-encoding m1Ψ mRNA treatment on T cell expansion. Naïve Thy1.2$^+$ C57BL/6 mice were immunized with MOG_{35-55} m1Ψ or U mRNA, and the expansion of both endogenous T cells and adoptively transferred MOG_{35-55}–T cell receptor transgenic Thy1.1$^+$ CD4$^+$ T cells from 2D2 mice (*8*) was assessed. Both MOG_{35-55}–encoding mRNAs induced proliferation of adoptively transferred CD4$^+$ 2D2 T cell, with MOG_{35-55} m1Ψ mRNA being superior (Fig. 1F). Similarly, endogenous MOG_{35-55}–specific CD4$^+$ T cells in naïve mice were expanded by both MOG_{35-55}–encoding mRNAs (Fig. 1G). However, the functional properties of the T cells induced with either of these mRNAs differed profoundly. MOG_{35-55} m1Ψ mRNA treatment was capable of expanding or inducing de novo Foxp3$^+$ regulatory T cells (T_{reg} cells) in both wild-type C57BL/6 and 2D2-Foxp3-eGFP transgenic mice (Fig. 1H and fig. S2A), whereas overall frequencies of CD4$^+$ Foxp3$^+$ T cells did not change (Fig. 1H). CD4$^+$ T cells from vaccinated 2D2 animals inhibited the in vitro proliferation of antigen-specific naïve CD4 T cells in a dose-dependent manner. By contrast, CD4$^+$ T cells of MOG_{35-55} U mRNA or control-treated mice showed little to no suppressive activity (fig. S2B).

We studied the cytokine response profiles upon in vitro antigen restimulation and the phenotypes of expanded T cells in repetitively vaccinated C57BL/6 mice in more detail. Whereas MOG_{35-55} U mRNA–expanded T cells exhibited a functional T_H1 effector profile with secretion of IFN-γ, tumor necrosis factor–α (TNFα), interleukin-6 (IL-6), granulocyte-macrophage colony-stimulating factor, and

Corrected 19 March 2021. See full text.

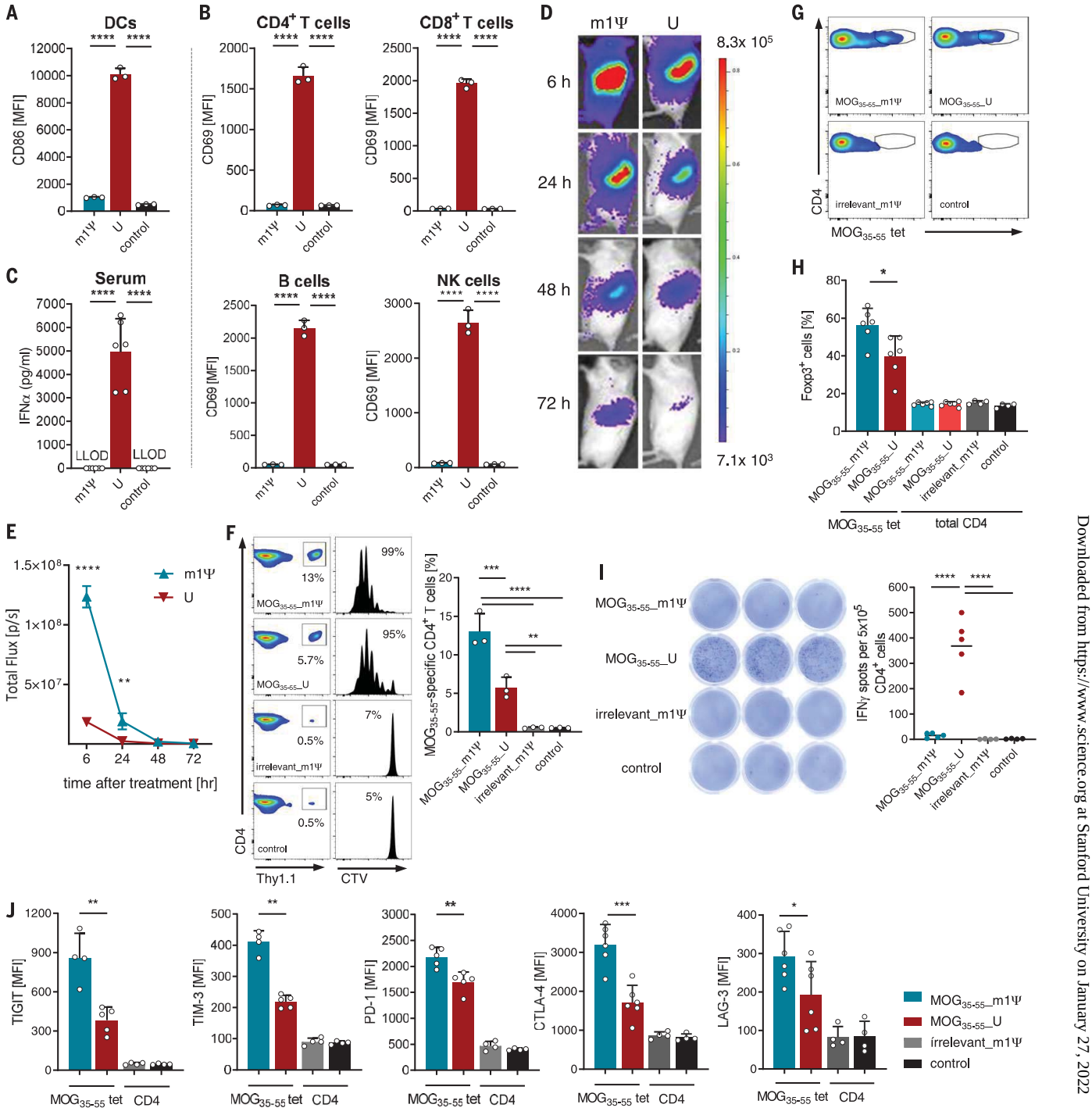

Fig. 1. Antigen-encoding m1Ψ mRNA potently expands antigen-specific CD4$^+$ T_{reg} cells by noninflammatory delivery into the spleen. (**A** and **B**) Activation of splenic immune cells 24 hours after (n = 3) and (**C**) IFN-α serum levels 6 hours after intravenous injection of LPX-formulated mRNAs and saline (control) in C57BL/6 mice (n = 6). (**D** and **E**) Bioluminescence imaging of albino C57BL/6 mice (n = 5) after intravenous injection of m1Ψ or U LUC mRNA. Representative mice are shown. (**F**) Frequency and proliferation profiles of MOG_{35-55}–specific CD4$^+$ T cells isolated from Thy1.1$^+$ 2D2 mice, cell trace violet (CTV)–labeled, and transferred into naïve Thy1.2$^+$ C57BL/6 recipient mice. Twenty-four hours after adoptive cell transfer, C57BL/6 mice were treated with mRNAs or saline (control). Mice were sacrificed on day 4, and spleens were analyzed for proliferating CD4$^+$ Thy1.1$^+$ cells (n = 3). (**G**) Expansion of endogenous MOG_{35-55}–specific CD4$^+$ T cells and (**H**) frequency of splenic Foxp3$^+$ T_{reg} cells (n = 6) in C57BL/6 mice after treatment (days 0, 3, 7, and 10) with mRNA or saline (control) analyzed by MOG_{35-55}–tetramer (tet) staining 3 days after last dosing (n = 4 to 6). (**I**) CD4$^+$ T cells of mice from (G) tested for IFN-γ secretion by enzyme-linked immune absorbent spot (ELISpot) upon restimulation with MOG_{35-55} peptide (n = 4 to 5). (**J**) Phenotype of tet$^+$ CD4$^+$ T cells of mice from (G). Data were compared by using one-way analysis of variance (ANOVA) and post hoc Tukey's test in (A) to (C), (F), and (I) or by unpaired two-tailed Student's t test in (H) and (J). Mean fluorescence intensity (MFI) of bulk CD4 T cells of control groups from (H) and (J) are depicted to show baseline expression levels. Error bars indicate mean ± SD. *$P \le 0.05$; **$P \le 0.01$; ***$P \le 0.001$; ****$P \le 0.0001$. LLOD, lower limit of detection.

Corrected 19 March 2021. See full text.

IL-2 (Fig. 1I and fig. S3), splenic $CD4^+$ T cells from MOG_{35-55} m1Ψ mRNA–treated mice did not secrete these proinflammatory cytokines, even when exposed to very high antigen concentrations. The only measurable factors were low levels of anti-inflammatory and T_H2 type–associated cytokines such as IL-10, IL-5, and IL-13 (fig. S3). The T cell exhaustion markers TIGIT, TIM-3, PD-1, CTLA-4, and LAG-3 were strongly up-regulated on MOG_{35-55} m1Ψ mRNA–expanded $tetramer^+$ T cells (Fig. 1J).

Exposure to m1Ψ mRNA does not impair the capability to mount immune responses

$CD11c^+$ APCs of mice first exposed to m1Ψ mRNA and thereafter injected with U mRNA did not show any impairment in their ability to respond to this TLR-agonistic stimulus with up-regulation of costimulatory molecules and IFN-α secretion (Fig. 2, A and B). To investigate whether the induction and expansion of MOG_{35-55}–specific $CD4^+$ T_{reg} cells affects de novo priming of antigen-specific immune responses, we exploited two broadly used model systems. First, C57BL/6 mice underwent prime-boost (days 6 and 13) vaccination with U mRNA encoding the ovalbumin (OVA) epitope SIINFEKL and were concurrently exposed to MOG_{35-55}–encoding m1Ψ mRNA (days 0, 3, 7, and 10). SIINFEKL-specific $CD8^+$ T cells were expanded above 40% of total blood $CD8^+$ T cells (Fig. 2C) and displayed properties of effector T (T_{eff}) cells such as cognate IFN-γ secretion and highly potent and antigen-specific killing (Fig. 2, D and E), which suggested uncompromised T cell priming and expansion. In a second experiment, mice were immunized intramuscularly with a self-amplifying RNA (saRNA) vaccine encoding influenza hemagglutinin (HA) (day 6) concurrent to repeated treatment with MOG_{35-55} m1Ψ mRNA or controls. Again, the capability of mice to mount a protective immune response and develop neutralizing antibodies was unimpaired (Fig. 2, F and G). Overall, both studies demonstrate that MOG_{35-55} m1Ψ mRNA–induced antigen-specific $CD4^+$ T_{reg} cells do not suppress functional immune responses against nonmyelin antigens.

Treatment with antigen-encoding m1Ψ mRNA ameliorates EAE in mice

Next, we studied the tolerogenic potential of MOG_{35-55} m1Ψ mRNA in C57BL/6 mice with MOG_{35-55}–induced EAE. Treatment with MOG_{35-55} m1Ψ mRNA was capable of blocking all clinical signs of EAE in mice (Fig. 3A), whereas control animals showed the typical course of the disease with rapid monophasic progression. In mice started on MOG_{35-55} m1Ψ mRNA treatment when a paralysis of the tail or beginning of the hindlimbs were noted (disease score of 1 to 2 of EAE), further disease progression could be prevented, and motor functions were restored (Fig. 3B and fig. S4A). This included occasional cases of reversion of paralysis, which was most likely attributable to an anti-inflammatory effect rather than tissue repair.

Various effects were observed in mice treated with antigen-encoding m1Ψ mRNA compared with control animals. In the brain and spinal cord, the total amount of infiltrating $CD4^+$ T cells, MOG_{35-55}–specific $CD4^+$ T cells and subsets of $CD4^+$ T cells secreting IFN-γ and IL-17A were considerably lower (Fig. 3, C, D, and F, and figs. S4B and S5). Demyelination of the spinal cord was also considerably reduced (Fig. 3E). In the spleen of MOG_{35-55} m1Ψ mRNA–treated animals, we observed an increase of lymphocytes (fig. S5), including MOG_{35-55}–specific $CD4^+$ T cells with low CD62L, CCR6, and CCR7 expression, and up-regulation of CD69 (fig. S6). CCR6, CCR7, and CD62L are critical for access of T cells to the central nervous system (CNS) (*9*–*12*), and the transmembrane C-type lectin CD69 is known to promote lymphocyte retention in the spleen (*13*).

Next, we analyzed the autoantigen-specific $CD4^+$ T cells in those mice in which the manifestation of EAE was prevented by treatment with MOG_{35-55} m1Ψ mRNA on days 7 and 10. MOG_{35-55}–specific splenic $CD4^+$ T cells from treated animals showed down-regulation of the activation marker CD44 and strong expression of coinhibitory molecules (Fig. 3G). At the peak of disease (day 16 after disease induction), CD5, ICOS, LAG-3, PD-1, CTLA-4, TIGIT, and TIM-3 were up-regulated in $tetramer^+$ splenic $CD4^+$ T cells. Furthermore, we detected a highly activated T_{reg} cell population (Fig. 3, H and I) and lower numbers of T_H1 and T_H17 MOG_{35-55}–specific $CD4^+$ T cells (Fig. 3H). Similar findings in mice with symptomatic EAE (disease score of 1 to 2 at start of treatment) further confirmed the potent disease-suppressive activity of antigen-encoding m1Ψ mRNA (fig. S4).

We extended our study of the preventive and therapeutic effect of m1Ψ mRNA to other EAE mouse models. The SJL model is based on autoreactivity against the $PLP_{139-151}$ epitope and is characterized by recurring EAE symptoms resulting in a relapsing-remitting disease, similar to the clinical presentation of MS in patients. Treatment of SJL mice with $PLP_{139-151}$ m1Ψ mRNA twice a week starting from day 7 after EAE induction resulted in almost full disease control (fig. S7A). Even when the mice were treated after the first disease peak (starting on day 14 after disease induction), progression of the disease was halted (fig. S7B).

Treatment with m1Ψ mRNA leads to therapeutically effective bystander tolerance

In another experimental setup, we addressed a key challenge in human MS, namely that antigen spread leads to a complex antimyelin autoreactivity pattern and the specificity of autoreactive T cell clones in individual patients, and thus, the potential targets for direct antigen-specific tolerization is unknown. A clinically viable approach would be to use bystander tolerance by inducing T_{reg} cells, which, once activated by their cognate antigen, would suppress T cells against other antigens in the inflamed tissue.

We evaluated bystander activity in two experimental settings. F1 C57BL/6 x SJL mice with $PLP_{139-151}$ peptide–induced EAE were vaccinated with m1Ψ mRNA encoding either $PLP_{139-151}$ (the disease-causing autoantigen), MOG_{35-55} (unrelated autoantigen, against which m1Ψ mRNA is capable of inducing potent effector T_{reg} cells), or irrelevant m1Ψ mRNA (Fig. 4A and fig. S7C). MOG_{35-55} m1Ψ mRNA treatment showed a dose-dependent therapeutic effect on EAE, similar to the curative effect mediated by vaccination with $PLP_{139-151}$ m1Ψ mRNA, indicating a strong T_{reg} cell–mediated bystander suppression, also given the fact that antigen spread has been described for this particular EAE model (*14*). Antigen-specific T_{reg} cells were notably expanded and highly activated, constituting >80% of de novo expanded MOG_{35-55}–specific $CD4^+$ splenic T cells (Fig. 4, B and C). T_{eff} cell infiltration into the brain and spinal cord in m1Ψ mRNA–treated mice was reduced (Fig. 4, D to F), and no signs of demyelination in the spinal cord were detected (Fig. 4G).

We also investigated a complex EAE model driven by multiple pathogenic autoreactive T cell clones against MOG_{35-55}, $PLP_{139-151}$, $PLP_{178-191}$, MBP_{84-104}, and $MOBP_{15-36}$, which could be successfully treated with the mixture of m1Ψ mRNAs coding for the corresponding four disease-inducing autoantigenic epitopes. m1Ψ mRNA encoding MOG_{35-55} were therapeutically almost as effective as those encoding the cocktail of all four disease targets. This suggests that even polyclonal autoimmune disease driven by a broad autoreactive T cell repertoire can be sufficiently controlled by m1Ψ mRNA targeting a strong bystander tolerance–mediating T cell epitope (fig. S7D).

One potential risk associated with antigen-specific tolerization is the induction of autoantibodies against respective targets, which can exacerbate disease (*15*). Moreover, nucleoside-modified mRNA is known to be highly immunogenic and to induce high antibody titers when formulated with immune stimulatory lipid nanoparticles (*16*). We therefore analyzed anti–MOG_{35-55} immunoglobulin G (IgG) antibody responses in the sera of EAE mice upon m1Ψ mRNA vaccination. First, we measured anti–MOG_{35-55} levels in sera of MOG_{35-55} peptide–induced EAE (C57BL/6 mice), which were vaccinated with MOG_{35-55} m1Ψ mRNA on days 7 and 10 after EAE induction. Anti–MOG_{35-55} IgG levels were not elevated in comparison with those of control animals treated

Corrected 19 March 2021. See full text.

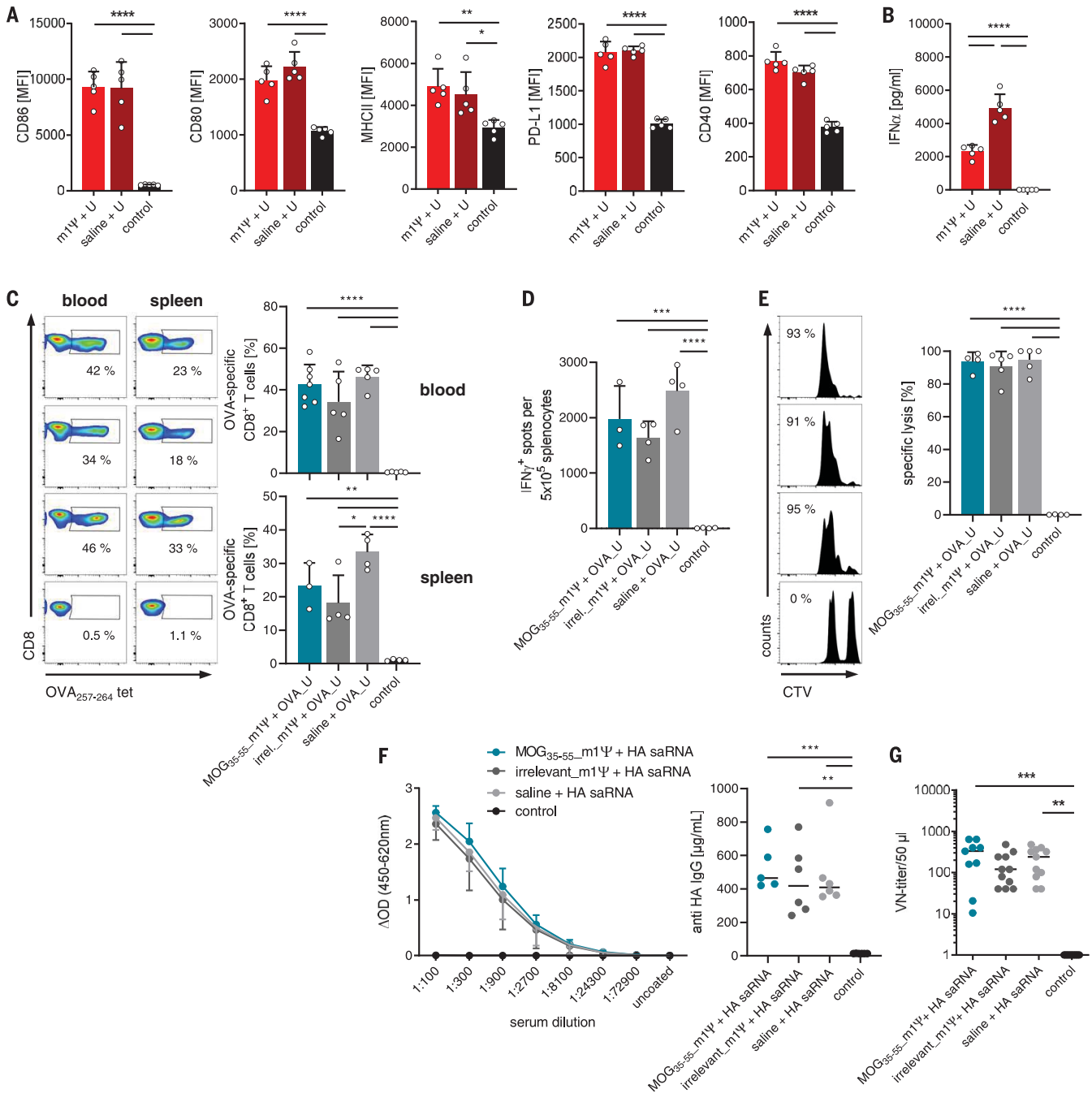

Fig. 2. Exposure to m1Ψ mRNA does not impair the capability to mount immune responses. (**A**) Activation of splenic CD11c$^+$ APCs 24 hours after (n = 3) and (**B**) IFN-α serum levels 6 hours after intravenous injection (day 3) of LPX-formulated U mRNA or saline (control) in C57BL/6 mice (n = 6), which were pretreated with m1Ψ mRNA or saline (control) at day 0. MHCII, major histocompatibility complex II. (**C** to **E**) De novo priming of SIINFEKL-specific CD8$^+$ T cells in C57BL/6 mice with prior exposure to MOG_{35-55} or irrelevant m1Ψ mRNA or saline (days 0, 3, 7, and 10) to SIINFEKL U mRNA prime-boost vaccination (days 6 and 13). Controls only received saline. (C) Frequency of SIINFEKL-specific CD8$^+$ T cells ($OVA_{257-264}$ tet) in blood (n = 5 to 7) and spleen (n = 3 to 4). (D) IFN-γ secretion was measured by ELISpot upon restimulation of total splenocytes of mice from (C) (n = 3 to 4) with SIINFEKL peptide and (E) in vivo antigen-specific killing of adoptively transferred CTV-labeled and peptide-loaded splenocytes of naïve mice (n = 4 to 5). For in vivo cytotoxicity assays, mice were adoptively transferred on day 18 with 0.5 µM (low) or 5 µM (high) CTV-labeled naïve splenocytes pulsed with peptide (6 µg/ml). Of these target cells, 1.5 × 10^6 cells were adoptively transferred into immunized and control recipients at a ratio of 1:1 (irrelevant $HA_{518-526}$ peptide–loaded CTV_{low}:SIINFEKL peptide–loaded CTV_{high}). Recipient splenocytes were recovered and analyzed by flow cytometry 18 hours after transfer, and antigen-specific lysis was determined as follows: specific lysis (%) = [1 − (percentage of cells pulsed with SIINFEKL/percentage of cells pulsed with HA) × 100]. (**F**) Total (n = 5 to 6) and (**G**) neutralizing (n = 9 to 11) anti-HA IgG in C57BL/6 mice with prior exposure to MOG_{35-55} or irrelevant m1Ψ mRNA or saline (days 0, 3, 7, and 10). Controls only received saline. Protective immune responses were measured 28 days after mice were immunized with influenza HA-saRNA (1 µg intramuscularly) on day 6. Data were compared by using one-way ANOVA and post hoc Tukey's test. Error bars, mean ± SD. ΔOD, change in optical density; VN, virus neutralizing.

Corrected 19 March 2021. See full text.

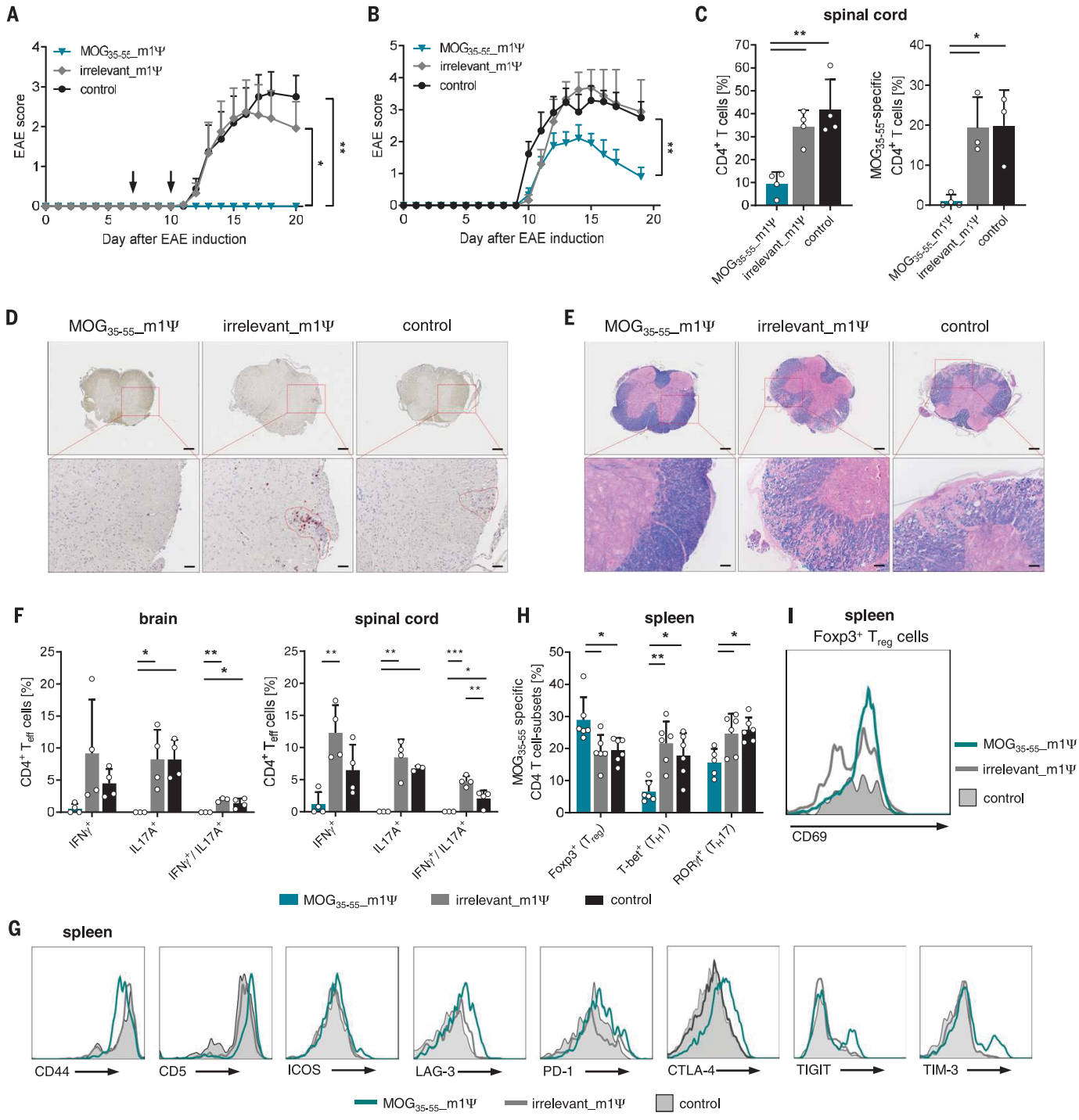

Fig. 3. Treatment with antigen-encoding m1Ψ mRNA ameliorates EAE in mice. (**A** and **B**) Disease severity in MOG_{35-55}–induced EAE (n = 6 to 8 C57BL/6 mice per group) treated with m1Ψ mRNA or saline (control) (A) on days 7 and 10 after disease induction or (B) when disease progressed to a score of 1 to 2. (**C**) Frequency of $CD4^+$ T cell and MOG_{35-55}–specific $CD4^+$ T cells in the spinal cord of mice treated on days 7 and 10 after disease induction (n = 3 to 4). $Thy1.1^+$ 2D2 $CD4^+$ T cells were transferred 1 day before EAE induction into $Thy1.2^+$ recipient mice and analyzed in the target organs on day 16 after disease induction. (**D**) Representative CD4 staining in the spinal cord of EAE mice treated with m1Ψ mRNAs or saline (control) (n = 3) on days 7 and 10 after disease induction and analyzed at day 16 after EAE induction. (**E**) Representative Luxol fast blue (LFB) staining revealing areas of demyelination in the spinal cord of mice from (D) (n = 3). (**F** to **I**) Frequency of $CD4^+$ IFN-γ– and IL-17A–secreting cells in brain and spinal cord (n = 3 to 4) (F) and flow cytometry analysis of splenic tetramer$^+$ $CD4^+$ T cells (n = 4 to 6) [(G) to (I)] of EAE mice treated with m1Ψ mRNAs or saline (control) on days 7 and 10 after disease induction and analyzed at day 16 after EAE induction. Area under the curve (AUC) was used to determine statistical significance through one-way ANOVA and Tukey's multiple comparison test of the different EAE disease development curves in (A) and (B). Data were compared by using one-way ANOVA and post hoc Tukey's test in (F) and (H). Error bars indicate mean ± SEM in (A) and (B) or mean ± SD in (C), (F), and (H). The scale bar in the upper row of (D) and (E) represents 200 μm and, in the lower row of (D) and (E), represents 50 μm.

Corrected 19 March 2021. See full text.

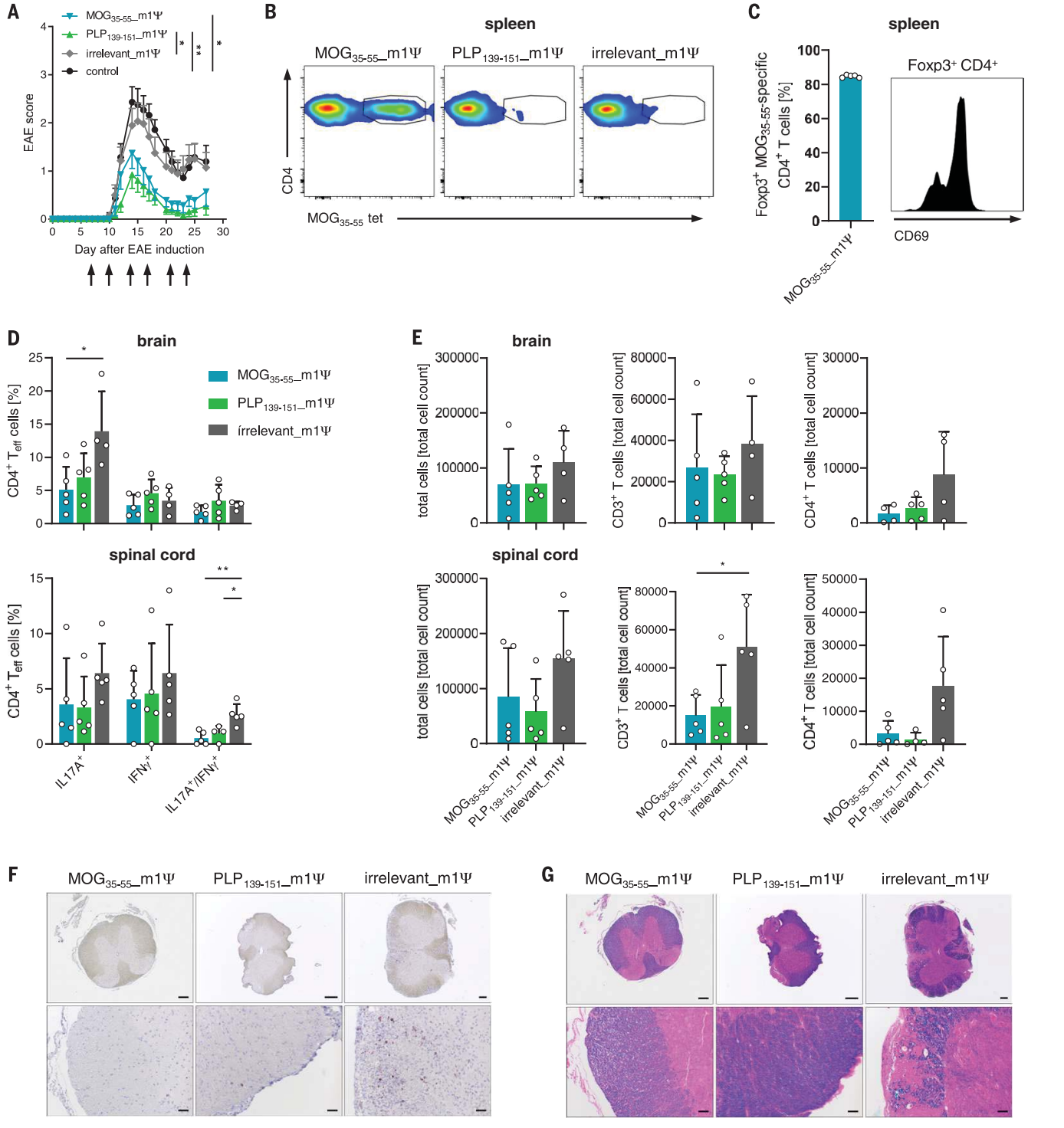

Fig. 4. Treatment with m1Ψ mRNA leads to therapeutically effective bystander tolerance. (**A**) Dynamics of EAE in $PLP_{139-151}$–induced EAE mice (n = 13 to 15 F1 C57BL/6 x SJL mice) upon treatment with MOG_{35-55} m1Ψ, $PLP_{139-151}$ m1Ψ, irrelevant m1Ψ mRNA, or saline (control) twice per week starting on days 7 and 10 after disease induction with 40 μg of m1Ψ mRNA. (**B** and **C**) Expansion of endogenous MOG_{35-55}–specific $CD4^+$ T cells (B) and frequency of $Tetramer^+$ $Foxp3^+$ T_{reg} cells and analysis of CD69 expression on respective cell population (C) upon treatment with m1Ψ mRNA measured in the spleen on day 28 after EAE induction (n = 5). (**D**) Frequency of $CD4^+$ IFN-γ– and IL-17A–secreting cells upon $PLP_{139-151}$–peptide restimulation and (**E**) total cell count of lymphocytes in brain and spinal cord of EAE mice treated with different m1Ψ mRNAs (n = 4 to 5) and analyzed on day 28 after EAE induction. (**F**) Representative CD4 staining in the spinal cord of EAE mice from (A) (n = 2). (**G**) Representative LFB staining revealing areas of demyelination in the spinal cord of mice from (A) (n = 2). AUC was used to determine statistical significance through one-way ANOVA and Tukey's multiple comparison test of the different EAE disease development curves (A). Data were compared by using one-way ANOVA and post hoc Tukey's test. Error bars indicate mean ± SEM in (A) or mean ± SD in (C) to (E). The scale bar in the upper row of (F) and (G) represents 200 μm and, in the lower row of (F) and (G), represents 50 μm.

Corrected 19 March 2021. See full text.

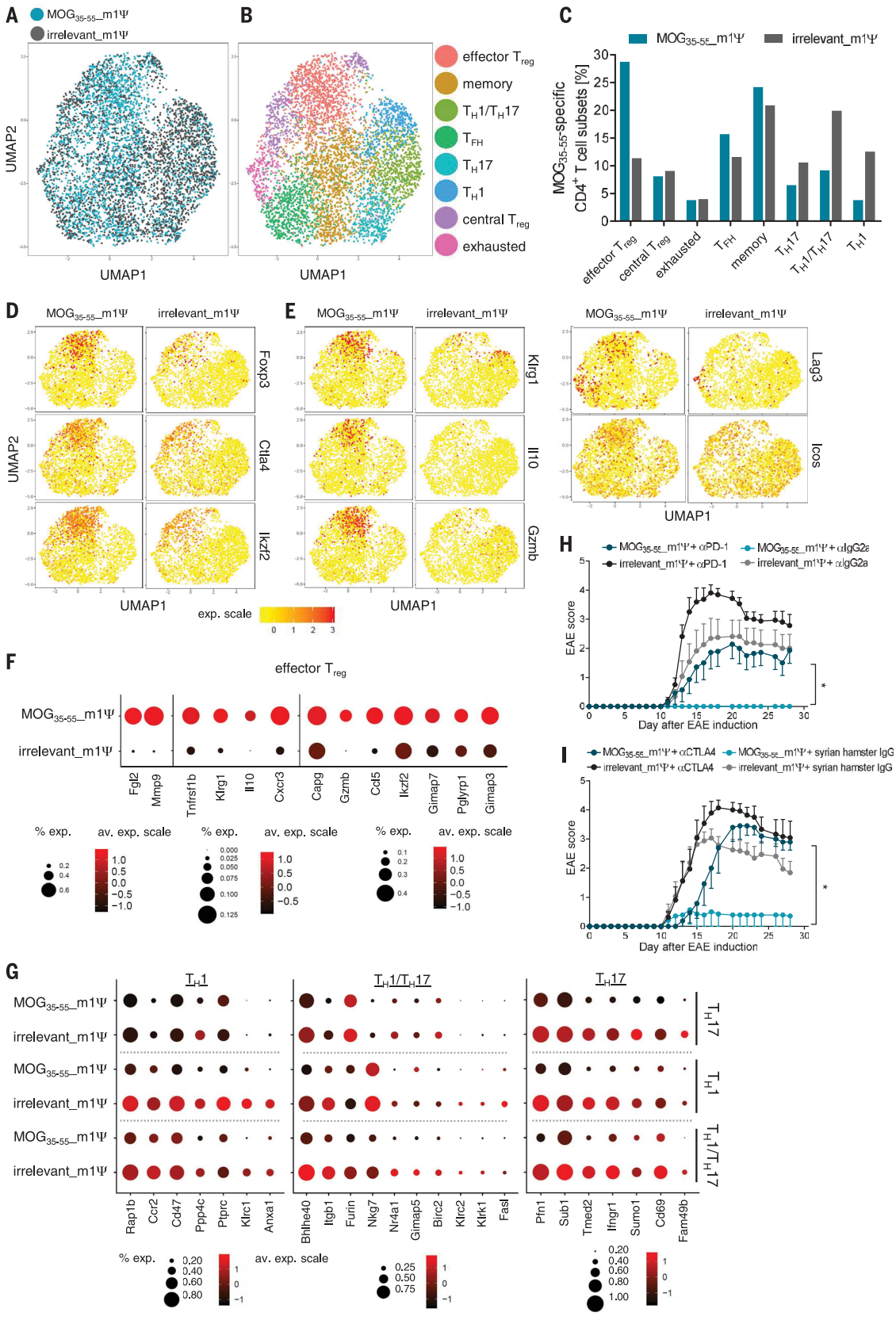

Fig. 5. Distinct splenic antigen-specific CD4$^+$ T cell subsets are expanded in EAE mice treated with antigen-encoding m1Ψ mRNA. (**A** to **G**) MOG_{35-55}–specific CD4$^+$ T cells isolated from mice with MOG_{35-55}–induced EAE treated with m1Ψ mRNA on days 7 and 10 after disease induction and analyzed by single-cell RNA sequencing on day 15 or day 16, respectively. (A) A two-dimensional uniform manifold approximation and projection (UMAP) projection of MOG_{35-55}–specific CD4$^+$ T cells isolated from different treatment groups (each dot represents one cell) identified by unsupervised clustering. (B) UMAP projection of single cells, color-coded according to the identified cell subsets. (C) Frequency of different cell subsets. (D) and (E) depict a UMAP projection of classical T_{reg} cell markers (D) and effector T_{reg} cell markers (E). (F) Genes up-regulated in an effector T_{reg} subpopulation upon MOG_{35-55} m1Ψ mRNA treatment (adjusted P value < 0.05). av. exp., average expression. (G) Genes down-regulated upon MOG_{35-55} m1Ψ mRNA treatment in T_H1, T_H17, and T_H1/T_H17 cell subsets (adjusted P value < 0.05). (**H** and **I**) MOG_{35-55}–induced EAE in C57BL/6 mice (n = 8 per group) treated with m1Ψ mRNA on days 7 and 10 after disease induction in combination with (H), anti–PD-1, and (I) anti–CTLA-4 blocking antibodies or isotype controls administered twice per week. Statistical significance of AUC differences of EAE disease development curves was assessed by using one-way ANOVA and Tukey's multiple comparison test in (H) and (I). Error bars represent mean ± SEM in (H) and (I).

Corrected 19 March 2021. See full text.

with irrelevant m1Ψ mRNA or saline (fig. S8A). This suggests that m1Ψ mRNA application does not exacerbate preformed autoantibody responses. Even after repetitive MOG_{35-55} m1Ψ mRNA challenge (twice per week, 12 times in total) of F1 C57BL/6 x SJL mice, no anti–MOG_{35-55} IgG antibodies were detected in those where EAE was induced with $PLP_{139-151}$–peptide immunization (fig. S8B).

Distinct antigen-specific CD4$^+$ T cell subsets are expanded in EAE mice treated with antigen-encoding m1Ψ mRNA

Next, we characterized the tolerized T cells by subjecting splenic tetramer$^+$ CD4$^+$ T cells from animals treated with MOG_{35-55} m1Ψ mRNA or irrelevant m1Ψ mRNA to single-cell RNA sequencing (table S1). Clustering analysis revealed eight distinct antigen-specific CD4$^+$ T cell subsets in EAE mice (Fig. 5, A and B, and fig. S9). The CD4$^+$ T cell identity of all subsets was confirmed with canonical T cell markers (fig. S10). We used sets of genes characterizing different functional T cell subphenotypes for further analysis (figs. S11 and S12). We identified two distinct populations sharing common T_{reg} cell markers (*Foxp3*, *Ikzf2*, and *Ctla4*). One of these subpopulations displayed typical effector T_{reg} cell markers (*Klrg1*, *Il10*, *Gzmb*, *Lag3*, and *Icos*), whereas the other subset were central T_{reg} cells as defined by markers *Sell* and *Bcl2* and low expression of the common effector-associated molecules (*17*, *18*) (figs. S11, A and B, and S13A). We also identified T_H1 (*Ifnγ* and *Tbx21*), T_H17 (*Il17a/f* and *Tmem176a/b*), and T_H1/T_H17 cells with combined expression of T_H1 and T_H17 markers (*Csf2*, *Tbx21*, *Ifnγ*, and *Il17a*). Moreover, we found exhausted antigen-specific T cells (*Lag3* and *Cd160*), T follicular helper (T_{FH}) cells (*Il4*, *Il21*, and *Cxcr5*), and a T cell cluster with a memory phenotype (*Ccr7*^{high} and *Tcf7*^{high}) (figs. S11, C to H, and S13, B and C).

The relative frequencies of these antigen-specific CD4$^+$ T cell subpopulations changed in EAE mice treated with antigen-encoding m1Ψ mRNA. Most notably, in animals treated with MOG_{35-55} m1Ψ mRNA, the effector T_{reg} cells constituted the largest cluster by frequency and cell count (Fig. 5C). The T_H1, T_H17, and T_H1/T_H17 T_{eff} cell subpopulations were strongly reduced in comparison with those of control animals treated with irrelevant m1Ψ mRNA, whereas exhausted T cell and central T_{reg} cell subpopulations were of similar size in both groups (Fig. 5C). We also found substantial differences in the expression levels of functionally relevant genes and activation markers. Common T_{reg} cell markers such as *Foxp3*, *Ikzf2*, and *Ctla4* were present in T_{reg} cell subpopulations of both treatment groups (Fig. 5D), whereas transcripts characteristic for effector T_{reg} cells and associated with T_{reg} cell suppressive function, such as *Klrg1*, *Il10*, *Gzmb*, *Lag3*, and *Icos*, were enriched in MOG_{35-55} m1Ψ mRNA–treated EAE mice and almost completely absent in those treated with irrelevant m1Ψ mRNA (Fig. 5, E and F). Likewise, the transcript profiles of the T_H1, T_H17, and T_H1/T_H17 T_{eff} cell clusters differed considerably between the two treatment groups (Fig. 5G and fig. S14A). The most prominent examples of differentially regulated genes were those involved in differentiation (*Anxa1*, *Ppp4c*, and *Mid1*) (*19*–*21*), migration (*Ccr2*, *Itgb1*, *Wdr26*, and *Rap1b*) (*22*–*26*) or cytokine production of T_{eff} cells (*Bhlhe40*) (*27*). In accordance with a previous study (*28*), we detected mainly down-regulation of genes associated with cell cycle and cell division in the mice treated with MOG_{35-55} m1Ψ mRNA (fig. S14B). The number of genes up-regulated in T_H1, T_H17, and T_H1/T_H17 T_{eff} cell subpopulations from MOG_{35-55} m1Ψ mRNA–treated mice was small (fig. S14A).

To visualize the relationships between the identified major cell populations, we performed single-cell trajectory analysis (fig. S15). Each state represents subpopulation structures of closely related transitory cellular states. T cells from mice treated with irrelevant m1Ψ mRNA appeared mainly as fully differentiated cells in state 5, representing T_H1, T_H17, and T_H1/T_H17 T_{eff} cells (fig. S15, B, D, and F). By contrast, T cells from the MOG_{35-55} m1Ψ mRNA–treated group were in state 1 (memory) or mainly differentiated in state 2, representing effector T_{reg} cells and T_{FH} cells (fig. S15, B, C, and F). In sum, these findings indicate that m1Ψ mRNA treatment rather than deleting autoreactive T cells tips the immunological balance in favor of suppression of disease promoting MOG_{35-55}–specific T_H1, T_H17, and T_H1/T_H17 T_{eff} cells by expanding effector T_{reg} cells.

PD-1 and CTLA-4 signaling contribute to the induction and maintenance of antigen-specific tolerance

Expression of coinhibitory receptors such as CTLA-4 and PD-1 on effector and T_{reg} cells is a key mechanism of immune homeostasis. We therefore assessed the mechanistic contribution of these pathways to antigen-specific tolerance mediated by m1Ψ mRNA. Treatment of EAE mice with MOG_{35-55} m1Ψ mRNA combined with anti–PD-1 or anti–CTLA-4 antibody on days 7 and 10 after EAE induction aggravated the disease in control groups in accordance with the known unleashing effect of checkpoint blockade on autoreactive T cells (*29*). Both CTLA-4 and PD-1 blockade almost completely abolished the EAE-protective effect of MOG_{35-55} m1Ψ mRNA (Fig. 5, H and I). Flow cytometry and single-cell RNA sequencing revealed almost exclusive and high expression of *Ctla4* by MOG_{35-55}–specific CD4$^+$ T_{reg} cells (fig. S16, A and B), which supports a role of this population for mediating tolerance. The effect of PD-1 blockade may be driven by two independent mechanisms, one being invigoration of preexistent T_{eff} cells and the other being the inhibition of the de novo induction of antigen-specific T_{reg} cells, which also depends crucially on PD-1 signaling (*30*). These findings suggest that disease-mediating T cells are suppressed but not deleted in mice treated with antigen-encoding m1Ψ mRNA and that both PD-1 and CTLA-4 signaling critically contribute to the induction and maintenance of antigen-specific tolerance.

Discussion

Our study describes nanoparticulate delivery of nucleoside-modified autoantigen-encoding mRNA into lymphoid CD11c$^+$ APCs as a therapeutic approach for antigen-specific tolerization. We show, at single-cell resolution, the generation of different antigen-specific CD4$^+$ T cell subpopulations with distinct functional states.

Selective delivery of autoantigens into CD11c$^+$ APCs resident in lymphoid tissues exploits a highly effective natural mechanism for induction and maintenance of peripheral tolerance. The presentation of autoantigens in a noninflammatory context leads to expansion of antigen-specific CTLA-4$^+$, ICOS$^+$, IL-10$^+$, and Foxp3$^+$ effector T_{reg} cells (*31*) that not only suppress antigen-specific autoreactive T_{eff} cells but also exert bystander immunosuppression, thereby enabling disease control even in a complex, polyclonal model of autoimmunity.

Bystander activity of T_{reg} cells has been associated with noncognate mechanisms depending on cell-cell interaction, such as secretion of suppressive factors, e.g., IL-10 and transforming growth factor–β (TGF-β) (*32*). Thus, one would expect that MOG-specific T_{reg} cells activated upon reexposure to their cognate antigen in the CNS would suppress immune responses that occur at that very location for a defined period of time. Because of its temporo-spatial nature, T_{reg} cell activity exerts tissue-specific immune regulation rather than pan-immune suppression (*33*). This is in line with prior studies indicating that T cell tolerance to tissue-restricted self-antigens is actively mediated by antigen-specific T_{reg} cells rather than deletion (*34*).

With the presented approach, key challenges for clinical translation of antigen-based treatment of autoimmune diseases can be addressed. Both the nucleoside-modified, purified mRNA and the liposomal nanoparticle formulation are pharmaceutically well-defined clinical-stage compounds and are currently being explored in human trials for various disease indications (*35*). The repetitive administration of m1Ψ mRNA is not compromised by induction of autoantigen-specific antibody responses, which usually causes safety-limiting constraints for other applications. Production of mRNA pharmaceuticals is fast and cost-efficient, and virtually any autoantigen can be encoded by

mRNA. Thus, tailoring the treatment for the disease-causing antigens of individual patients is conceivable, similar to that which has been successfully executed in the setting of personalized cancer vaccines (*36*, *37*). Combination of m1Ψ mRNAs encoding either multiple personalized autoantigens or autoantigens that confer bystander tolerance may enable control of even complex autoimmune diseases.

REFERENCES AND NOTES

1. P. Serra, P. Santamaria, *Nat. Biotechnol.* **37**, 238–251 (2019).
2. A. Miller, O. Lider, H. L. Weiner, *J. Exp. Med.* **174**, 791–798 (1991).
3. L. M. Kranz *et al.*, *Nature* **534**, 396–401 (2016).
4. K. Karikó, M. Buckstein, H. Ni, D. Weissman, *Immunity* **23**, 165–175 (2005).
5. K. Karikó *et al.*, *Mol. Ther.* **16**, 1833–1840 (2008).
6. K. Karikó, H. Muramatsu, J. Ludwig, D. Weissman, *Nucleic Acids Res.* **39**, e142 (2011).
7. N. Yogev *et al.*, *Immunity* **37**, 264–275 (2012).
8. E. Bettelli *et al.*, *J. Exp. Med.* **197**, 1073–1081 (2003).
9. I. S. Grewal *et al.*, *Immunity* **14**, 291–302 (2001).
10. Y. Arima *et al.*, *Cell* **148**, 447–457 (2012).
11. A. Reboldi *et al.*, *Nat. Immunol.* **10**, 514–523 (2009).
12. S. Noor, E. H. Wilson, *J. Neuroinflammation* **9**, 77 (2012).
13. L. R. Shiow *et al.*, *Nature* **440**, 540–544 (2006).
14. R. Gold, C. Linington, H. Lassmann, *Brain* **129**, 1953–1971 (2006).
15. C. P. Genain *et al.*, *Science* **274**, 2054–2057 (1996).
16. N. Pardi *et al.*, *Nat. Commun.* **9**, 3361 (2018).
17. E. Cretney, A. Kallies, S. L. Nutt, *Trends Immunol.* **34**, 74–80 (2013).
18. R. J. Miragaia *et al.*, *Immunity* **50**, 493–504.e7 (2019).
19. N. Paschalidis *et al.*, *J. Neuroinflammation* **6**, 33 (2009).
20. S. A. Apostolidis, T. Rauen, C. M. Hedrich, G. C. Tsokos, J. C. Crispín, *J. Biol. Chem.* **288**, 26775–26784 (2013).
21. A. Collison *et al.*, *Nat. Med.* **19**, 232–237 (2013).
22. E. E. Kara *et al.*, *Nat. Commun.* **6**, 8644 (2015).
23. B. T. Fife, G. B. Huffnagle, W. A. Kuziel, W. J. Karpus, *J. Exp. Med.* **192**, 899–906 (2000).
24. S. Glatigny, R. Duhen, M. Oukka, E. Bettelli, *J. Immunol.* **187**, 6176–6179 (2011).
25. C. Runne, S. Chen, *Cell Adh. Migr.* **7**, 214–218 (2013).
26. T. Kinashi, K. Katagiri, *Immunol. Lett.* **93**, 1–5 (2004).
27. C. C. Lin *et al.*, *Nat. Commun.* **5**, 3551 (2014).
28. B. R. Burton *et al.*, *Nat. Commun.* **5**, 4741 (2014).
29. L. M. Yshii, R. Hohlfeld, R. S. Liblau, *Nat. Rev. Neurol.* **13**, 755–763 (2017).
30. L. Wang *et al.*, *Proc. Natl. Acad. Sci. U.S.A.* **105**, 9331–9336 (2008).
31. N. Ohkura, S. Sakaguchi, *Nat. Immunol.* **12**, 283–284 (2011).
32. A. M. Thornton, E. M. Shevach, *J. Immunol.* **164**, 183–190 (2000).
33. X. Clemente-Casares *et al.*, *Nature* **530**, 434–440 (2016).
34. F. P. Legoux *et al.*, *Immunity* **43**, 896–908 (2015).
35. N. Dammes, D. Peer, *Trends Pharmacol. Sci.* **41**, 755–775 (2020).
36. U. Sahin, Ö. Türeci, *Science* **359**, 1355–1360 (2018).
37. U. Sahin *et al.*, *Nature* **547**, 222–226 (2017).

ACKNOWLEDGMENTS

We thank V. Ames, K. Zwadlo, A. Plaschke, I. Beulshausen, E. Petscherskich, E. Daniel, R. Roth, B. Jesionek, M. Brkic, A. Selmi, M. Baiersdörfer, and S. Berl for technical assistance; S. Witzel, B. Tillmann, S. Wurzel, Z. Yildiz, and N. Blaumeuser for cloning of constructs; S. Fesser, K. Tillmann, J. Beckerle, E. Heintz, and C. Golletz for mRNA production; and P. Guna, A.-L. Popa, and H. Haas for providing liposomes. Additional support was provided by S. Attig and A. Hohberger for cell sorting. Moreover, we acknowledge F. Vascotto for support and scientific discussion for the manuscript, T. Regen for experimental advice, and L. Giese for supporting single-cell RNA sequencing. Furthermore, we thank the NIH Tetramer Core Facility for providing the MOG_{35-55} MHC class II tetramer. **Funding:** This work has been supported by grants from the Immunology Research Center (FZI) Mainz (FZI-TRP 2014-12 to U.S. and N.Y.) and the Deutsche Forschungsgemeinschaft DFG (SFB/CRC-TR 128 to A.W.). **Author contributions:** U.S. was responsible for conception and experimental strategy of the study. Planning and analysis of the experiments were done by C.K., L.M.K., M.D., S.Kr., H.B., and J.P., supported by N.Y. and A.W. C.K. and S.Ki. performed immunological experiments. Processing and analysis of scRNA-seq data was done by L.K., E.D., and M.S., supported by T.B. Ö.A.-Ö. performed IHC experiments. C.K., Ö.T., and U.S. interpreted the data and drafted the manuscript. L.K., E.D., M.S., M.D., K.K., and A.W. supported writing of the manuscript. All authors edited and approved the final manuscript. **Competing interests:** L.M.K., H.B., K.K., Ö.T., and U.S. are employees at BioNTech SE (Mainz, Germany). M.D. and S.Kr. work as consultants for BioNTech SE (Mainz, Germany). C.K., J.P., L.M.K., M.D., S.Kr., K.K., and U.S. are inventors on patents and patent applications related to this study. Ö.T. and U.S. are stock owner and management board members of BioNTech SE (Mainz, Germany). All other authors declare no competing interests. **Data and materials availability:** Correspondence and request for materials should be addressed to U.S. The single-cell RNA-seq data have been deposited at the European Nucleotide Archive (ENA) under the accession number PRJEB43603.

SUPPLEMENTARY MATERIALS

science.sciencemag.org/content/371/6525/145/suppl/DC1
Materials and Methods
Figs. S1 to S16
Tables S1 and S2
References (*38*–*52*)

View/request a protocol for this paper from *Bio-protocol*.

13 June 2019; resubmitted 27 April 2020
Accepted 17 November 2020
10.1126/science.aay3638

A noninflammatory mRNA vaccine for treatment of experimental autoimmune encephalomyelitis

Christina KrienkeLaura KolbElif DikenMichael StreuberSarah KirchhoffThomas BukurÖzlem Akilli-ÖztürkLena M. KranzHendrik BergerJutta PetschenkaMustafa DikenSebastian KreiterNir YogevAri WaismanKatalin KarikóÖzlem TüreciUgur Sahin

Science, 371 (6525), • DOI: 10.1126/science.aay3638

Precision therapy for immune tolerance

Autoimmune diseases, such as multiple sclerosis (MS), result from a breach of immunological self-tolerance and tissue damage by autoreactive T lymphocytes. Current treatments can cause systemic immune suppression and side effects such as increased risk of infections. Krienke *et al.* designed a messenger RNA vaccine strategy that lacks adjuvant activity and delivers MS autoantigens into lymphoid dendritic cells. This approach expands a distinct type of antigen-specific effector regulatory T cell that suppresses autoreactivity against targeted autoantigens and promotes bystander suppression of autoreactive T cells against other myelin-specific autoantigens. In mouse models of MS, the vaccine delayed the onset and reduced the severity of established disease without showing overt symptoms of general immune suppression.

Science, this issue p. 145